JMEPEG (2018) 27:3255–3267
https://doi.org/10.1007/s11665-018-3427-2

1059-9495/$19.00

Texture Evolution in an Al-Cu-Mg Alloy During Hot Rolling

Peng Xia, Zhiyi Liu, Wenting Wu, Qi Zhao, Luqing Lu, and Song Bai

(Submitted January 25, 2018; in revised form April 16, 2018; published online May 25, 2018)

The texture evolution in the intermediate (the 1/4 thickness) layer of hot-rolled Al-Cu-Mg alloy sheets was investigated by the x-ray diffraction technique, electron backscattered diffraction analysis and transmission electron microscopy observation. The results showed that a texture transition from the shear texture {001}<110> to the β-fiber textures occurred as the rolling temperature increased to 420 °C. The shear strain caused by friction resulted in this strong shear texture formation at the low rolling temperature. As the rolling temperature increased, the plane strain substituting the shear strain dominated in the intermediate layer, giving rise to a significant increase in the β-fiber textures. Increasing the rolling temperature was found to preferentially activate the non-octahedral {112}<110> slip system, thereby benefiting the development of strong Brass. At the low rolling reduction of 74%, the textures with low intensity tended to converge on the α-fiber, containing Goss, Brass, P and L components. As the rolling reduction increased to 90%, the textures were strengthened and gradually flew toward the β-fiber, containing Brass, Copper and S components. The S and Copper bands were found to be the preferential sites for the development of recrystallizing Cube grains during hot rolling.

Keywords Al-Cu-Mg alloy, Cube grain, hot rolling, non-octahedral slip, texture evolution

1. Introduction

An important characteristic of thermomechanical processing in polycrystalline materials is the formation of deformation textures. The evolution of textures in aluminum alloys during hot deformation has been extensively investigated in recent decades (Ref 17). It has been known that the hot rolling textures include rolling components and recrystallized components (Ref 1). The rolling components in aluminum alloy textures mainly consist of the β-fiber textures containing Copper {112}<111>, S {123}<634> and Brass {011}<211>. Besides, Goss {110}<001> was also observed during hot deformation (Ref 2, 3). The fiber connecting between Goss, Brass, P {011}<122> and L {110}<011> is the so-called α-fiber. Recrystallization textures generally include Cube, Goss and P. However, it was reported that the recrystallized components of hot rolling textures mainly consisted of the Cube component (Ref 2, 4, 5).

The effect of deformation temperature on the texture evolution of aluminum has been studied by Panchanadeeswaran et al. (Ref 2, 6). It was reported that an overall increase in rolling textures was found in the deformed material at elevated temperatures (Ref 2). While Liu et al. (Ref 6) revealed that at high deformation temperatures initial orientations were more easily rotated to the β-fiber between the Brass and S orientations than to the Copper orientation. Besides the temperature, strain rate was also considered to play an important role in the texture evolution. The combined effect of the two factors can be expressed by Zener–Hollomon (Z) parameter (Ref 7), which is given by: $Z = \dot{\varepsilon}\exp(Q/RT_{\mathrm{D}})$. Maurice et al. (Ref 5) revealed that the Cube component in the polycrystal material increased when the Z parameter reduced. The low Z value means high temperature or low strain rates. Samajdar et al. (Ref 8) found that a decrease in Z value reduced the relative increase in the Copper and S components. In addition, the initial texture and alloy phase composition were considered to have substantial impacts on the formation of the final deformation textures (Ref 2, 3, 9, 10). The Copper texture preferentially formed in the deformed purity aluminum with the random initial texture, while the initial texture with the Cube orientation benefited the formation of a near Brass texture (Ref 2). Engler et al. (Ref 3) revealed that the pure aluminum after the plane compression often showed a Copper-type texture while the alloy with fine shearable particles represented relatively strong Goss and Brass textures (Ref 3, 9, 10).

Besides these common rolling textures mentioned above, the infrequent shear texture {001}<110> in deformation materials attracted less attention. This shear texture caused by the shear deformation was commonly observed in the surface layer of the material (Ref 11-13). Tian et al. (Ref 12) revealed that the rolling texture showed a remarkable decrease as the shear texture covers the surface for the heavy cold-rolled Cu-45at% Ni alloy tapes. It was report that the work hardening and friction force between the rolls and the material were responsible for the formation of the shear texture (Ref 12). Kang et al. (Ref 13) found that the hot rolling without lubrication led to the evolution of the pronounced through-thickness texture gradients and a strong shear texture was present in the surface region. These investigations mentioned above mainly focused on the intensity gradient of the shear texture along the thickness direction but paid scarcely any attention on the deformation temperature effecting on the shear texture development.

In view of previous researches mainly focusing on the texture evolution in the center layers of rolled sheets, while the shear texture {001}<110> is difficult to develop in the center layer, this investigation mainly aimed at the texture evolution in the intermediate (the 1/4 thickness) layer of hot-rolled Al-Cu-

Peng Xia, Zhiyi Liu, Wenting Wu, Qi Zhao, Luqing Lu, and **Song Bai**, Key Laboratory of Nonferrous Metal Materials Science and Engineering, Ministry of Education, Central South University, Changsha 410083, China; and School of Material Science and Engineering, Central South University, Changsha 410083, China. Contact e-mail: liuzhiyi335@163.com.

Mg alloy sheets. The texture compositions of the hot-rolled sheets at different rolling temperatures were measured in order to detect the general developing trend of rolling textures. Using a modified method first proposed by Shin et al. (Ref 14), the activated slip system during the hot rolling deformation could be identified to explain the formation of strong Brass at the high rolling temperature. Besides the rolling temperature, the influence of rolling reduction on the texture development was also discussed. Furthermore, the small quantity of recrystallized Cube grains was distinguished from the large deformation bands by electron backscattered diffraction (EBSD) analysis. In this way, the development of recrystallized Cube grains during hot rolling was well explored.

2. Experimental

The material used in this investigation was an Al-Cu-Mg aluminum alloy, whose nominal chemical composition is 4.0% Cu, 1.4% Mg, 0.6% Mn, 0.02%Ti, 0.06% Fe and 0.06% Si (in wt.%). The Al-Cu-Mg alloy ingot block with a thickness of 50 mm was cut from the raw ingot casting along the direction of pouring. The homogenization treatment of 495 °C/24 h was employed before hot rolling. The ingot blocks were rolled to the reduction of 90% at lubrication condition. The employed rolling temperatures contained 380, 400, 420, 440, 460, 480 and 495 °C. At the rolling temperature of 420 and 495 °C, the ingot blocks were additionally rolled to the reductions of 74, 82%. All the rolled sheets cooled in the water after hot rolling. The texture compositions of the 1/4 thickness layers of rolling sheets were measured by the x-ray diffraction (XRD) technique. The (111), (200) and (220) pole figures were examined by the Schulz back-reflection method using CuK_{α} radiation. The orientation distribution functions (ODFs) were calculated from the incomplete pole figures using the series expansion method ($l_{max} = 16$). The ODFs were presented as plots of constant φ_2 sections with isointensity contours in Euler space defined by the Euler angles φ_1, Φ and φ_2. Volume fractions of measured ideal orientations were calculated by integration within 15° of the ideal orientation peaks. Transmission electron microscopy (TEM) observation and corresponding selected area electron diffraction (SAED) analysis for the hot-rolled sheets in the intermediate layer were conducted by a Tecnai $G^2$20 microscope with an operating voltage of 200 kV. EBSD samples were prepared by mechanical grind, and electropolishing in a solution of 90% ethanol and 10% perchloric acid. All EBSD experiments were performed on a FEI Helios Nanolab 600i field emission gun scanning electron microscope with an accelerating voltage of 20 kV.

3. Results

3.1 Initial Texture Measurement

Figure 1 shows the representative ODF sections of the homogenized Al-Cu-Mg alloy. It can be observed that the initial texture presented a random distribution with a low intensity.

3.2 The Texture Development Influenced by the Rolling Temperature

Figure 2 illustrates the representative ODF sections in the intermediate layer of hot-rolled Al-Cu-Mg alloy sheets at various finish rolling temperatures (T_f). The start rolling temperature was 440 °C, and the finish temperatures of the hot-rolled sheets were measured by an infrared radiation thermometer with an error range of about 5 °C. The different finishing temperatures could be obtained by heating the rollers to different temperatures. The texture intensity distributions along the β-fiber of the hot-rolled Al-Cu-Mg alloy sheets with various finish rolling temperatures are present in Fig. 3. At the low T_f of 250 °C, corresponding orientation intensity $f(g)$ of Brass, Copper and S was 4.7, 1.8 and 3.9, respectively. While at the high T_f of 350 °C, corresponding orientation intensity $f(g)$ of the three textures reach 8.3, 7.7 and 10.2, respectively, as shown in Fig. 3. Obviously, elevating T_f could promote the enhancement of the β-fiber textures containing Brass, Copper and S. Besides, it was noted that the Brass component showed a larger increase than Copper and S with increasing T_f. This indicated that Brass was more sensitive to the finishing rolling temperature. Based on the above, it can be found that the finishing rolling temperature indeed played an important role in the texture development during the hot rolling. Considering that elevating T_f was in favor of the formation of the strong β-fiber textures, the subsequent rolling experiments were carried out under the condition of heating the rollers, so as to finish the rolling at high temperatures. In this investigation, when the roller temperature kept at 250 °C, the finish rolling temperatures of the sheets whose start rolling temperatures ranged from 380 to 495 °C were all not inferior to 350 °C. The higher start rolling temperature corresponded to the higher finish rolling

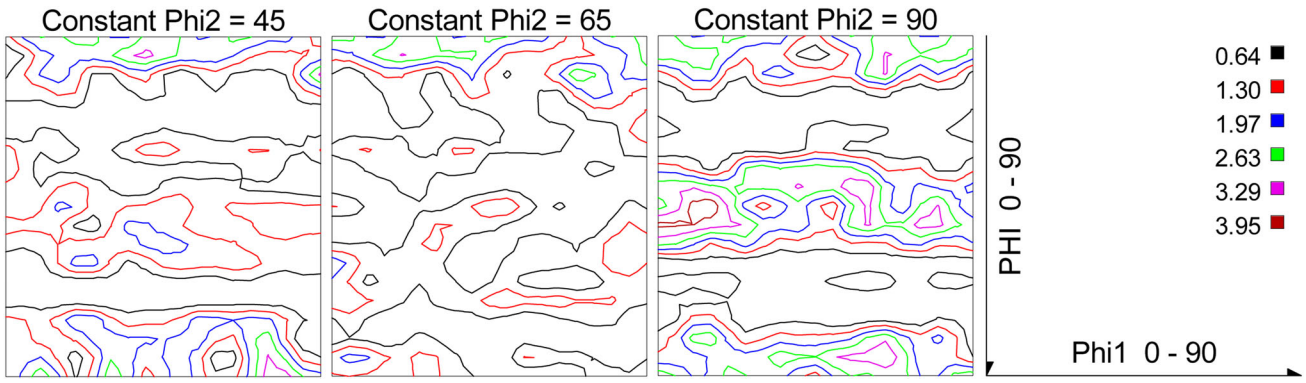

Fig. 1 Representative ODF sections of the homogenized Al-Cu-Mg alloy

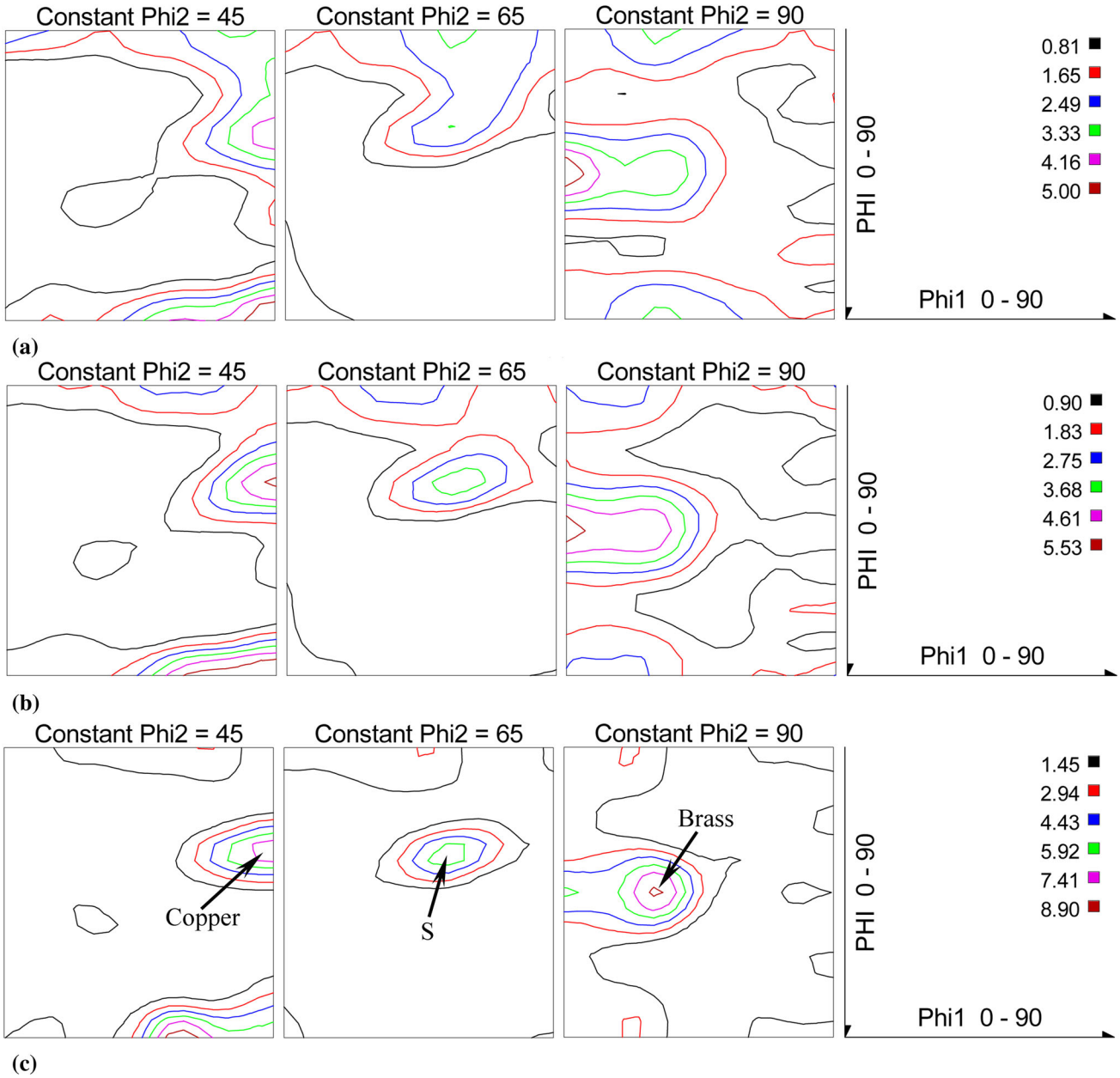

Fig. 2 Representative ODF sections in the intermediate layer of hot-rolled Al-Cu-Mg alloy sheets with various finish rolling temperatures: (a) T_f = 250 °C, (b) T_f = 300 °C and (c) T_f = 350 °C

temperature. In the subsequent rolling experiments, the start rolling temperature was taken as the rolling temperature, whose effect on the texture evolution was explored.

Figure 4 shows the representative ODF sections in the intermediate layer of hot-rolled Al-Cu-Mg alloy sheets at different rolling temperatures. Figure 5 illustrates the volume fraction changes of various textures with the increasing rolling temperature. One significant phenomenon can be found that the shear texture $\{001\}<110>$ was dramatically strong at the rolling temperature of 380 °C, with the large volume fraction of 23%, but when the rolling temperature increased to 420 °C, the volume fraction of the shear texture decreased to zero, as shown in Fig. 5. Meanwhile, when the rolling temperature increased from 400 to 420 °C, the volume fractions of the β-fiber textures containing Brass, Copper and S all increased sharply. It suggested that there was a texture transition from the shear texture to the β-fiber textures in the intermediate layer between 400 and 420 °C. When the rolling temperature rose to the higher level, the Brass component kept an increasing trend on the whole. At the rolling temperature of 495 °C, the volume fraction of Brass reached 26%. In contrast, the strength of Copper and S showed no evident changes with the rolling temperature increasing, and the corresponding volume fraction of Copper and S was 10.6 and 11.9%, respectively, as shown in Fig. 5. It indicated that elevating temperature was in favor of the formation of Brass. Besides, the emergence of Cube component at the high rolling temperature (not inferior to 420 °C) indicated the occurrence of recrystallization.

Figure 6 shows the representative ODF sections in the surface layer of rolled Al-Cu-Mg alloy sheets at different

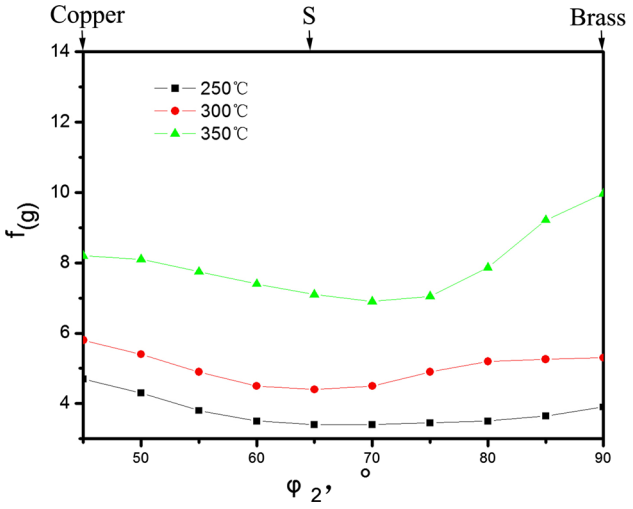

Fig. 3 Texture intensity distributions along the β-fiber of hot-rolled Al-Cu-Mg alloy sheets with various finish rolling temperatures

rolling temperatures. The intensity of shear texture in the surface layer was apparently stronger than that in the intermediate layer, as shown in Fig. 6(a). It indicated that the shear texture owned an intensity gradient along the thickness direction. Figure 6(b) shows that a relatively weak shear texture remained in the surface layer, suggesting that the shear texture caused by surface friction was difficult to be eliminated.

Figure 7 represents the bright-field TEM micrographs and corresponding SAED patterns in the intermediate layer of hot-rolled Al-Cu-Mg alloy sheets. As shown in Fig. 7(a), in the sheet rolled at 380 °C, the deformation band consisting of some dislocation substructures distributed along the <211> direction. In the hot-rolled sheets at 420, 460 and 495 °C, the deformation band with the direction of <111> could be observed, as shown in Fig. 7(b), (c) and (d). Besides, it is worth noting that the sheets hot rolled at high temperatures showed lower dislocation densities and some distinct subgrains developed in these sheets, as shown in Fig. 7(c) and (d). It implied that an appreciable dynamic recovery occurred during high-temperature rolling. From the SAED patters shown in Fig. 7, it can be observed that the sheets rolled at relatively low temperatures showed sharpened diffraction spots while the sheets rolled at high temperatures showed more scattered diffraction spots. The formation of subgrains in high-temperature rolling sheets promoted an increased misorientation, resulting in this scattered diffraction spot emerging. Shin et al. (Ref 14) provided a method to identify the activated slip systems. This method proposes that the direction of the deformation band should be parallel to the intersecting line between the slip plane and the viewing plane and should be normal to the selected zone axis (<110>, in this work). Thus, the direction of the deformation band is equivalent to that of the projection of the slip plane on the view plane. Accordingly, it can be inferred that the deformation band distributing along <211> direction indicates the activation of {111}<110> slip system while the deformation band remaining parallel to the <111> direction means the activation of non-octahedral {112}<110> slip system. Hence, the existence of deformation bands along the <111> direction, as shown in Fig. 7(b), (c) and (d), indicated that the slip system {112}<110> was more easily to operate at relatively high deformation temperatures.

3.3 Texture Development Influenced by the Rolling Reduction

Figure 8 shows the representative ODF sections in the intermediate layer of hot-rolled Al-Cu-Mg alloy sheets with different rolling reductions at the rolling temperature of 420 °C. Figure 9 illustrates the texture intensity distributions of hot-rolled sheets along the α-fiber and the β-fiber. It can be observed that the textures mostly located at the α-fiber containing Goss, Brass, P and L in the hot-rolled sheet with the low reduction of 74%. Corresponding texture intensity $f(g)$ of Copper, S and Brass was 2.8, 1.9 and 3.7, respectively. In contrast, as the rolling reduction increased, the textures gradually flew toward the β-fiber orientations containing Copper, S and Brass. The corresponding texture intensity $f(g)$ of Copper, S and Brass reaches 8.4, 9.2 and 9.1, respectively, at the rolling reduction of 90%, as shown in Fig. 9.

The texture evolution of hot-rolled Al-Cu-Mg alloy sheets at 495 °C as a function of the rolling reduction is shown in Fig. 10 and 11. At the high rolling temperature of 495 °C, it can be more clearly observed that the transition of texture distribution from the α-fiber to the β-fiber occurred with the increasing rolling reduction. As compared to the low rolling temperature of 420 °C, the entire texture intensity was enhanced distinctly. It can be found that the strong Brass component developed at the low rolling reduction of 74% while the Copper and S components showed much lower intensities. The corresponding texture intensity $f(g)$ of Copper, S and Brass at the rolling reduction of 74% was 3.9, 2.3 and 16.4, respectively. Then as the rolling reduction increases, the Brass component decreased to some extent but the whole intensity of the β-fiber textures appeared an increasing trend. Corresponding texture intensity $f(g)$ of Copper, S and Brass reaches 8.2, 7.8 and 10.4, respectively, at the rolling reduction of 90%, as shown in Fig. 11. In contrast with the relatively weak Brass developing at the low rolling temperature, as shown in Fig. 8, the higher intensity Brass forming at the high temperature in Fig. 10 again confirmed that elevating temperature could promote the formation of the Brass component.

3.4 The Cube Component in the Rolling Textures

The texture distribution maps of hot-rolled Al-Cu-Mg alloy sheets were acquired by EBSD analysis, as shown in Fig. 12. It can be observed that the S and Copper components existed in the sheets rolled at 380 °C, but the Brass and Cube components were absent, as shown in Fig. 12(d). It is well understood that the absence of Cube component should be attributed to the low rolling temperature. At the high rolling temperature, the occurrence of recrystallization during hot rolling brought about the Cube component developing in the hot-rolled sheet, as shown in Fig. 12(e) and (f). These recrystallized Cube grains can be divided into two types. One type of Cube grains was elongated, as shown in Fig. 12(e). In contrast, another type of Cube grains was approximately equiaxed with small sizes, as shown in Fig. 12(f). The elongated Cube grains probably nucleated during the previous rolling pass and then grew up but were flattened to a critical thickness in subsequent rolling passes, as proposed by Daaland et al. (Ref 4). It was noted that

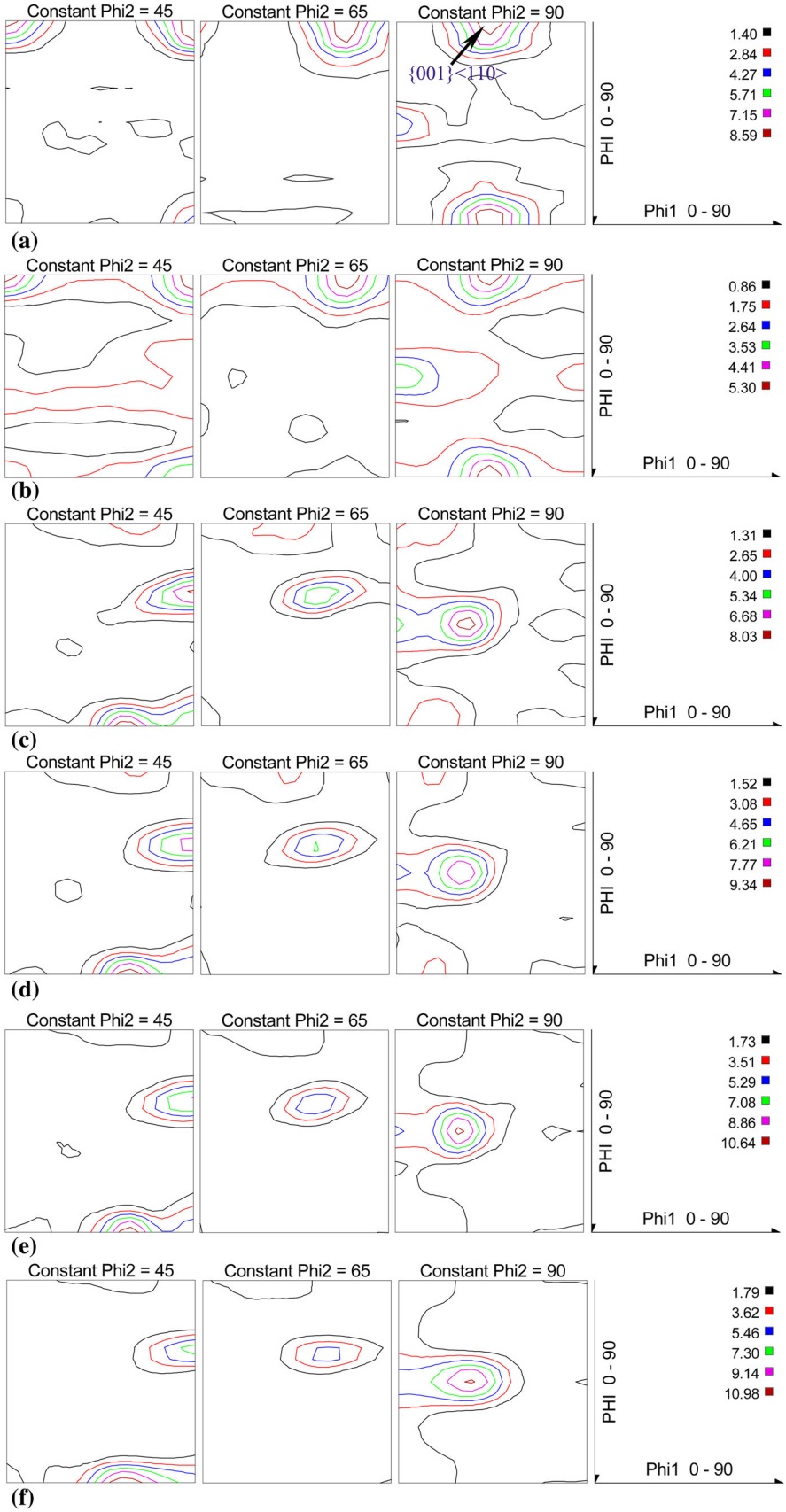

Fig. 4 Representative ODF sections in the intermediate layer of hot-rolled Al-Cu-Mg alloy sheets at various rolling temperatures: (a) 380 °C, (b) 400 °C, (c) 420 °C, (d) 460 °C, (e) 480 °C and (f) 495 °C

the small and near equiaxed Cube grains tended to appear in S or Copper bands, as shown in Fig. 12(f). This was consistent with the previous investigations (Ref 15, 16) proposing that S and Copper bands were preferential nucleation sites for Cube grains.

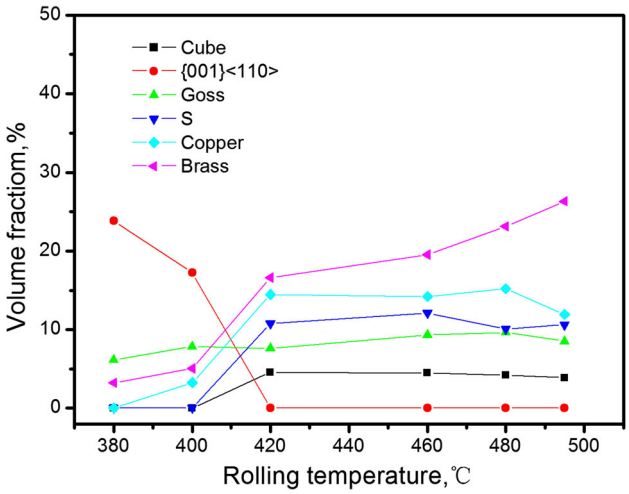

Fig. 5 Volume fractions of various textures of rolled Al-Cu-Mg alloy sheets at different rolling temperatures

4. Discussion

4.1 Development of the Shear Texture {001}<110>

Tian et al. (Ref 12, 13) revealed that the friction condition was an important factor effecting on the formation of the shear texture $\{001\}<110>$. It was reported that the shear strain caused by the severe friction developing between rolls and the rolled sheet brought about the strong shear texture in the surface layer. In this investigation, the shear texture was observed in the intermediate layer at the low rolling temperature (inferior to 420 °C) but disappeared at the high rolling temperature, as shown in Fig. 4. It indicated that the rolling temperature should have a significant influence on the development of the shear texture.

During hot rolling deformation of polycrystalline material, the plane strain occurs in all layers from sheet surface to the sheet center, but the large shear strain only occurs in the surface layer while in the center layer the shear strain is zero, as shown in Fig. 13(a). In other words, the shear strain represents an intensity gradient from the sheet surface to the sheet center. Different strains bring about the development of different textures. The large shear strain in surface layers leads to the formation of strong shear texture. In contrast, in the center layer, the dominant plane strain gives rise to the development of strong β-fiber textures, as show in Fig. 13(b). From the macro-texture measurement result, the shear texture disappeared while the β-fiber textures increased remarkably as the rolling temperature increased to 420 °C, as shown in Fig. 4(c). It suggested that the plane strain should start to displace the shear

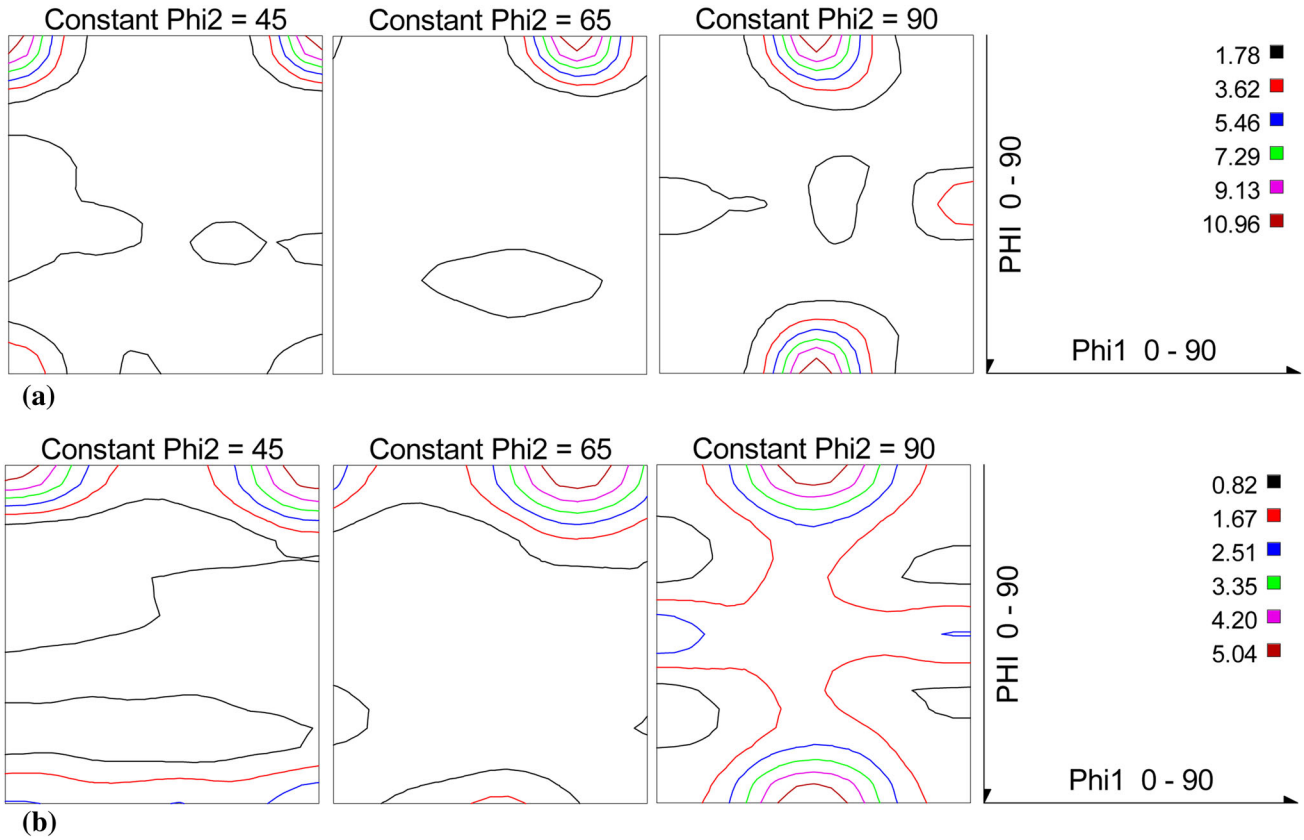

Fig. 6 Representative ODF sections in the surface layer of hot-rolled Al-Cu-Mg alloy sheets at different rolling temperatures: (a) 380 °C, (b) 420 °C

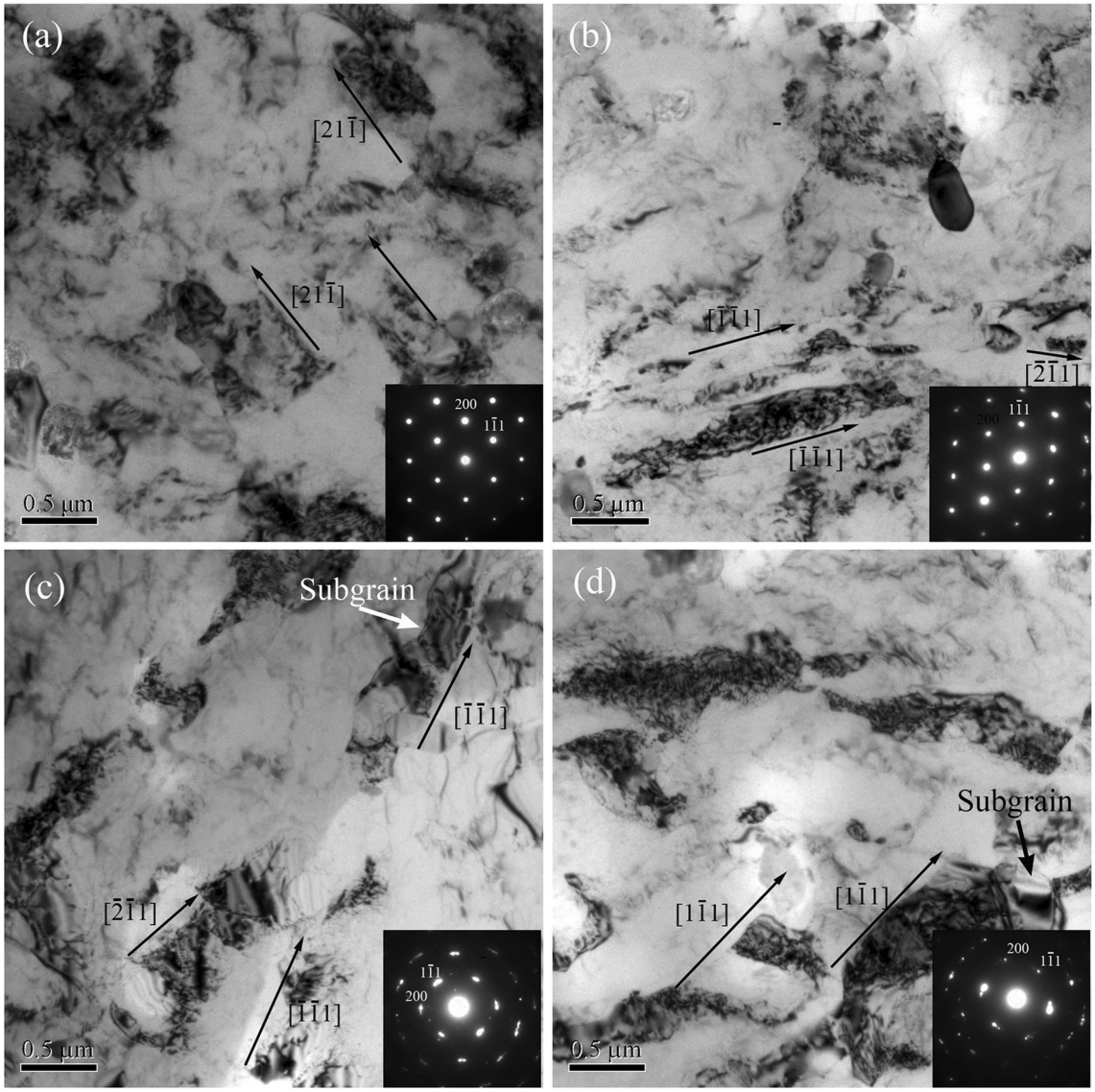

Fig. 7 TEM bright-field micrographs and corresponding SAED patterns of hot-rolled Al-Cu-Mg alloy sheets at different rolling temperatures: (a) 380 °C, (b) 420 °C, (c) 460 °C and (d) 495 °C

strain at a temperature between 400 and 420 °C in the intermediate layer. From Fig. 6(a), it can be found that the shear texture in the surface layer was stronger than that in the intermediate layer. It suggested that there was an intensity gradient for the shear texture existing in the thickness direction. Figure 6(b) shows that the shear texture remained in the surface layer even though the rolling temperature increased to 420 °C, suggesting that the shear texture was difficult to avoid in the surface layer. However, considering that the shear texture disappeared in the intermediate layer at 420 °C, it can be implied that the penetration depth of the shear texture would decrease if the rolling temperature increases.

For the idealized plane strain, the strain rate tensor $\dot{\varepsilon}_{ij} = 0$, when $i \neq j$. For practical rolling condition, the roll gap geometry and friction result in a nonzero $\dot{\varepsilon}_{13}$. Considering that the rolling is a two-dimensional problem, $\dot{\varepsilon}_{22} = \dot{\varepsilon}_{12} = \dot{\varepsilon}_{23} = 0$, the displacement gradient tensor $\dot{e}_{ij}$ can be summarized as:

$$\dot{e}_{ij} = \begin{pmatrix} \dot{e}_{11} & 0 & \dot{e}_{13} \\ 0 & 0 & 0 \\ \dot{e}_{31} & 0 & \dot{e}_{33} \end{pmatrix} \quad \text{(Eq 1)}$$

The shear strain $\dot{\varepsilon}_{13} = \frac{1}{2}(\dot{e}_{13} + \dot{e}_{31})$. The shear rate $\dot{e}_{31}$ is induced by the roll gap geometry while the shear rate $\dot{e}_{13}$ is induced by the friction effect between the rolled sheet and roll surface. As mentioned before, the shear texture is induced by the shear strain, while the shear strain contains two parts induced, respectively, by the roll gap geometry and friction (Ref 17-19). In this work, considering the invariable roll gap geometry, the magnitude of shear strain is determined by the friction. It has been proved that the friction coefficient was highly sensitive to the temperature (Ref 20-23). In the relatively low-temperature range, the friction coefficient increases as the temperature rises (Ref 20, 21). However, it will drop

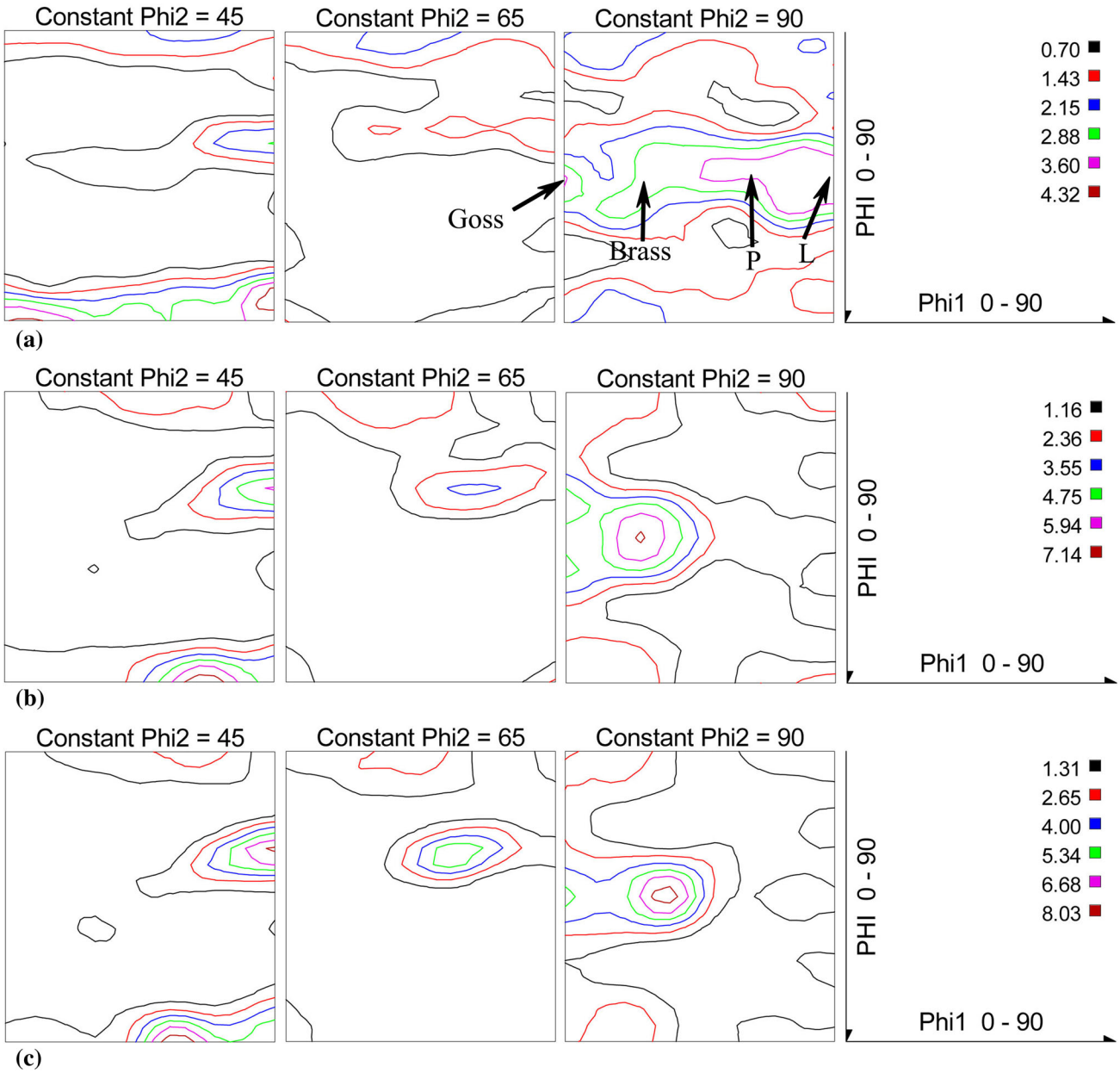

Fig. 8 Representative ODF sections in the intermediate layer of rolled Al-Cu-Mg alloy sheets at the rolling temperature of 420 °C with different rolling reductions: (a) 74%, (b) 82% and (c) 90%

when the temperature reaches a high level (Ref 22). Lenard (Ref 23) revealed that elevating the friction coefficient in flat rolling for commercially pure aluminum strips showed a declining trend when the temperature was higher than 300 °C. Considering all rolling processes were carried out at relatively high temperatures (not inferior to 350 °C), it can be inferred that the friction coefficient should decrease with the increasing rolling temperature. Yang et al. (Ref 24) revealed that the elevating friction coefficient could increase the shear strain under the constant roll gap geometry condition. It means that a small friction coefficient at the high rolling temperature could reduce the intensity of the shear strain, consequently resulting in a small penetration depth of the shear texture. Hence, it is well understood that the texture transition from the shear texture to the β-fiber textures occurred in the intermediate layer as the rolling reduction increased.

4.2 Development of the β-Fiber Textures

The effect of strain rate $\dot{\varepsilon}$ and deformation temperature T_D on the rolling textures can be expressed by Zener–Hollomon (Z) parameter (Ref 7), which is given by: $Z = \dot{\varepsilon}\exp(Q/RT_D)$. The $\dot{\varepsilon}$in this investigation can be regarded as a constant, while Z decreases as the deformation temperature increases. It was revealed that a low Z value promotes the formation of high-strength β-fiber textures (Ref 6, 25). Samajdar et al. (Ref 8) found that a decrease in Z value reduced the relative increase in the Copper and S components. This is in accordance with the result shown in Fig. 4 and 5. Duckham et al. (Ref 26) revealed that the formation of strong β-fiber textures was attributed to a healing out of the dislocations within the subgrains and a consumption of subgrains with scattered orientations during the dynamic recovery. For the metal with a high fault energy, the

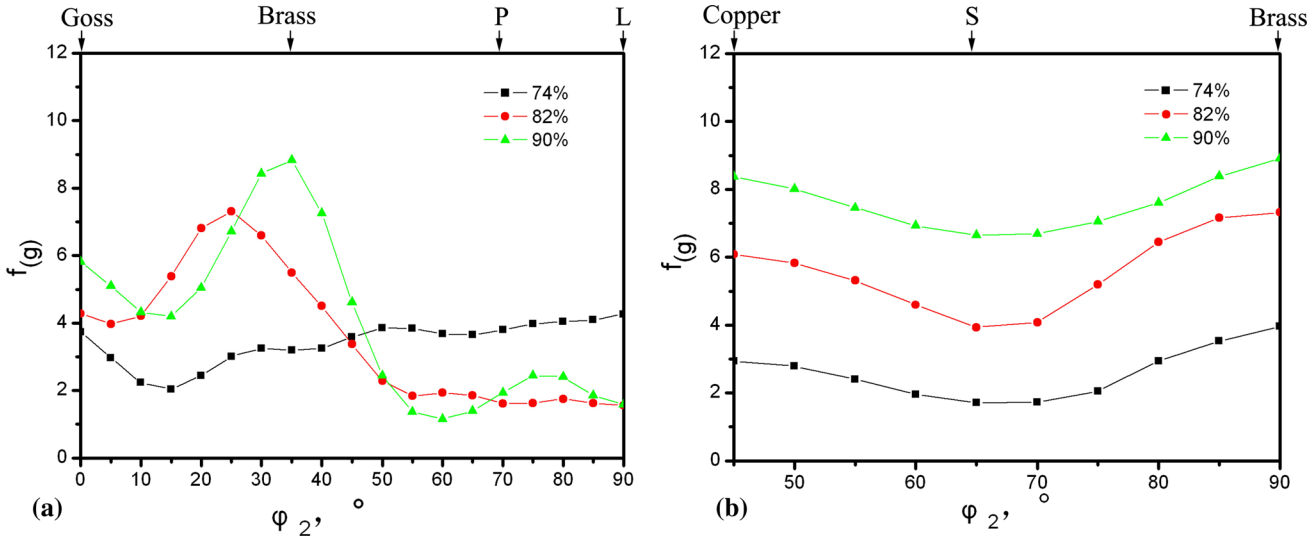

Fig. 9 Texture intensity distributions of the sheets rolled at 420 °C with different rolling reductions: (a) along the α-fiber, (b) along the β-fiber

dynamic recovery can be strengthened if the deformation temperature increases. It means that high deformation temperatures are in favor of the development of β-fiber textures. In this work, evident dynamic recovery occurring in the high-temperature rolling sheets, as shown in Fig. 7(c) and (d), should facilitate the strong β-fiber textures formation. In this work, the overall strength of β-fiber textures enhanced as the rolling temperature increased, as shown in Fig. 5. However, it can be found that the Brass component showed a larger increase as compared to the S and Copper components when the rolling temperature went up. This means that Brass should have a higher sensitivity to deformation temperature.

Contrepois et al. (Ref 9) found that the strong Brass texture was favored at high temperature. It was noted that the non-octahedral slip system $\{112\}<110>$ was more easily to be activated at high deformation temperatures, as shown in Fig. 7. Maurice et al. (Ref 5) used non-octahedral slip systems to simulate the evolution of hot rolling textures. A nonlinear function referring to the slip rate γ^k and the resolved shear stress τ^k on a system k was proposed to express the slip behavior (Ref 9, 27, 28):

$$\tau^k = \tau_0^k \left(\frac{\dot{\gamma}^k}{\dot{\gamma}_0^k} \right)^m \qquad \text{(Eq 2)}$$

where $\tau_0^k$and $\dot{\gamma}_0^k$ are reference quantities and m is the strain rate sensitivity parameter, given as: $m = \frac{\partial \ln \sigma}{\partial \ln \dot{\varepsilon}}$, and $0 < m < 1$. The temperature exerts influence on the slip through this m parameter. For aluminum alloys, the value of m goes up with the increasing temperature. When the temperature reaches 400-500 °C, m will range from 0.1 to 0.3 (Ref 9, 27). For the low m value, τ_0^k can be considered as equivalent as the value of critical resolved shear stress (CRSS). Maurice et al. (Ref 5, 29) revealed that the CRSS for the non-octahedral slip on {112} planes was roughly equal to that for the octahedral slip on {111}, {110} and {100} planes when the temperature reaches 0.7 T_m or higher. Consequently, the deformation at the high temperature was dominated by a mixture of {112} and {111} slip. Furthermore, for the hot rolling of polycrystalline material, a macroscopic shear ε_{12} dominated by $\{111\}<110>$ slip increased the shear strain incompatibilities. It was reported that the activation of the slip on {112} plane could facilitate the development of the Brass orientation (Ref 9, 28). Meanwhile, the macroscopic shear ε_{12} would decrease as this non-octahedral slip operated. This would significantly reduce the shear strain incompatibilities and in turn stabilize the Brass component at high temperature. In summary, increasing the temperature can easily activate the non-octahedral {112} plane slip and benefit the development of high-intensity Brass texture.

In our previous work (Ref 30), it was found that the rolling textures mainly converged on the orientation of Brass in the large hot deformation (rolling reduction > 95%). In the moderate deformation (rolling reduction: 70-90%), the α-fiber textures containing Goss, Brass, P and L preferred to develop in small deformation, while with the rolling reduction increasing, the textures tended to flow toward the β-fiber orientations containing Brass, Copper and S, as shown in Fig. 8 and 10. It suggested that the β-fiber textures had a higher stability at the large deformation than the α-fiber textures. It was mentioned that the texture stability was determined by the magnitude of substructural energy densities (E_v) of the grains or subgrains with this texture orientation (Ref 30-32). One grain or subgrain with lower substructural energy density means higher stability for its orientation. The equation of estimating the substructural energy density was given as (Ref 30, 31): $E_v = \frac{2}{\delta}\gamma$, where δ is the subgrain size, and γ is the stored energies of the subgrain which can be calculated by the well-known Read–Shockley equation (Ref 33). The result in previous work (Ref 30) showed that Brass, Copper and S grains always had lower substructural energy densities as compared to Goss and P grains after high deformations (rolling reduction > 70%). This can be used to explain the fact that the texture transition from the α-fiber textures to the β-fiber textures occurred with the strain increasing. Besides, it was noted that at the low temperature of 420 °C, the α-fiber textures developing in advance at the low strain presented a uniform distribution, as shown in Fig. 8(a). In contrast, at the high rolling temperature of 495 °C, the prior developed α-fiber textures mainly focused on the near Brass

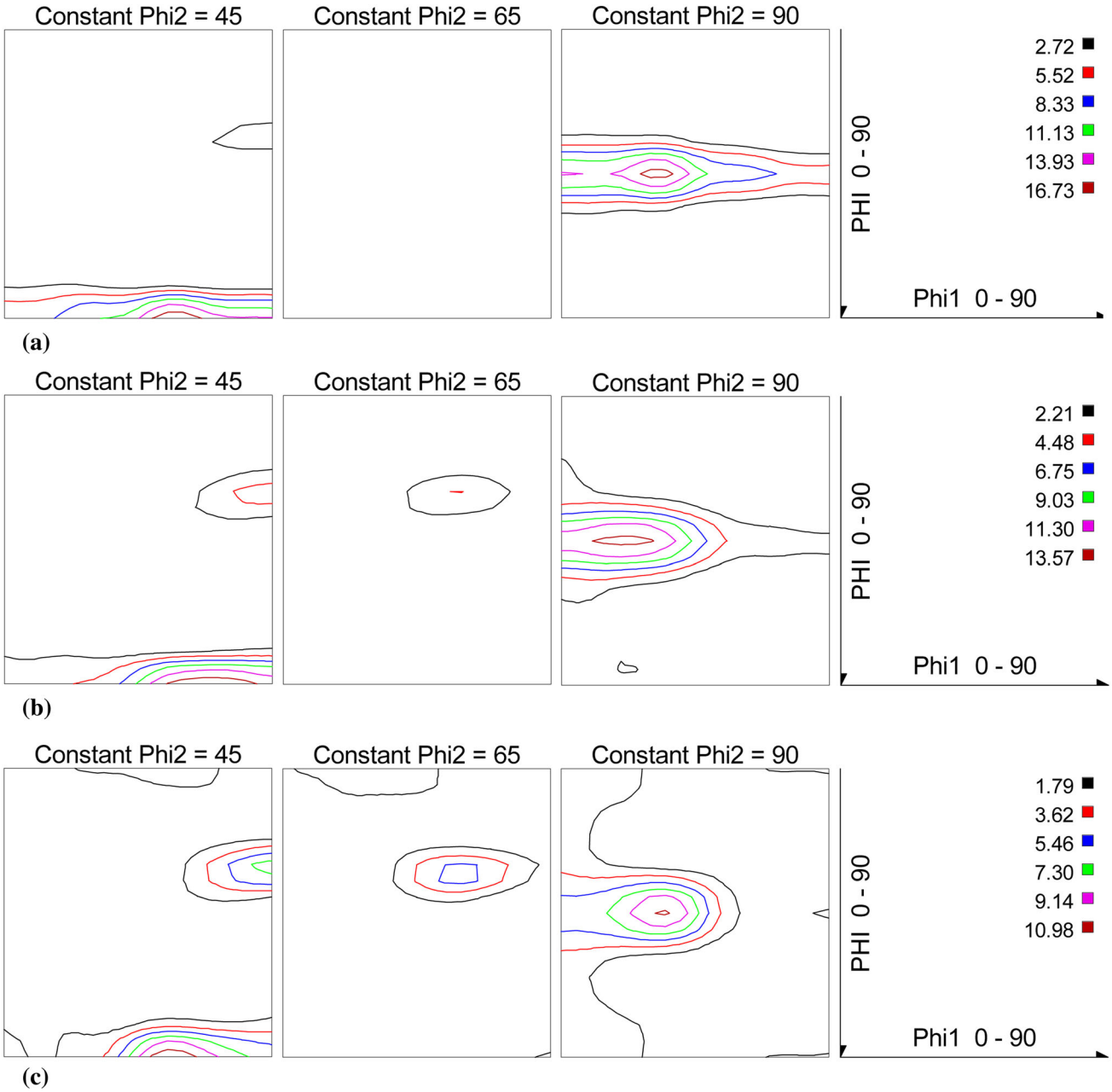

Fig. 10 Representative ODF sections of rolled Al-Cu-Mg alloy sheets at the rolling temperature of 420 °C with different rolling reductions: (a) 74%, (b) 82% and (c) 90%

orientation, as shown in Fig. 10(a). This should be attributed to the high temperature benefiting the formation of Brass. Above all, it can be seen that both the rolling temperature and the strain magnitude had important influences on the development of rolling textures. Compared to Copper and S, Brass was more sensitive to the two parameters in this study. On the one hand, a distinct Brass was able to be observed only at an enough large strain as shown in Fig. 8. On the other hand, when the rolling temperature was elevated, the strong Brass could develop prior to the other textures at a relatively small strain as shown in Fig. 10. In other words, it can be summarized that the large strain and the high deformation temperature facilitated the development of Brass. However, it needs to be pointed out that the strong Brass only developed at enough high rolling temperatures (not inferior to 420 °C) as shown in Fig. 4. At low deformation temperature of 380 °C, Brass was difficult to obtain even though the roll reduction was enough high, as shown in Fig. 4(a). It means that the rolling temperature should play a decisive role in the development of Brass as compared to the strain. This is mainly because that the high temperature prompted the operation of specific non-octahedral slip system, benefiting the formation of Brass as mentioned above. It was noted that Brass component decreased slightly as the rolling reduction increases as shown in Fig. 11. This should be attributed to the gradual decline of deformation temperature

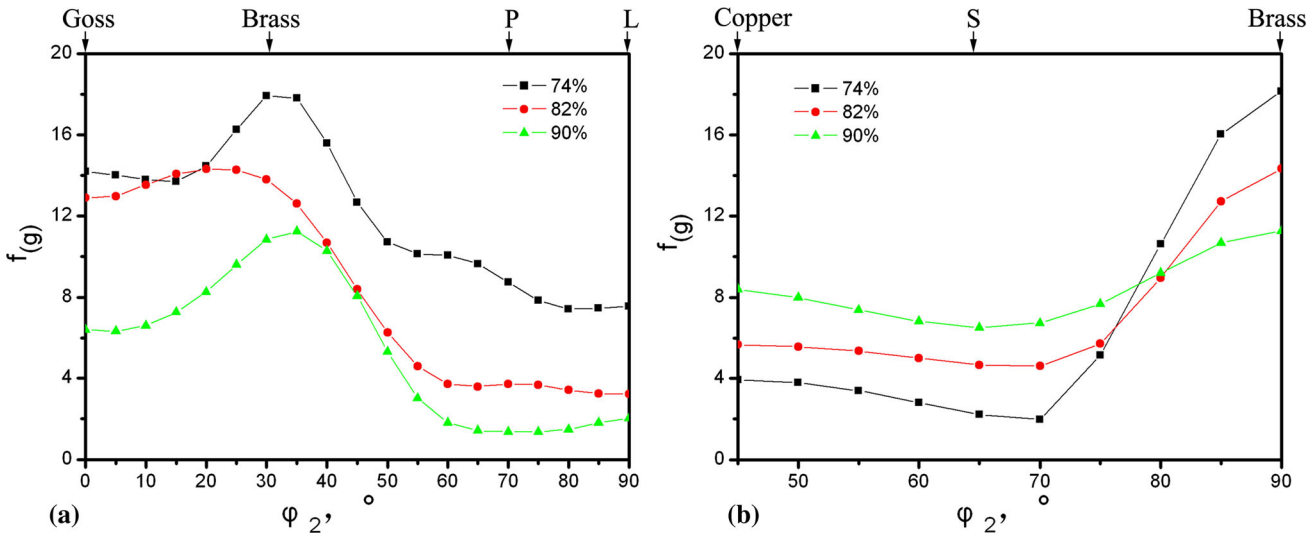

Fig. 11 Texture intensity distributions of rolled sheets at 495 °C with different rolling reductions: (a) along the α-fiber, (b) along the β-fiber

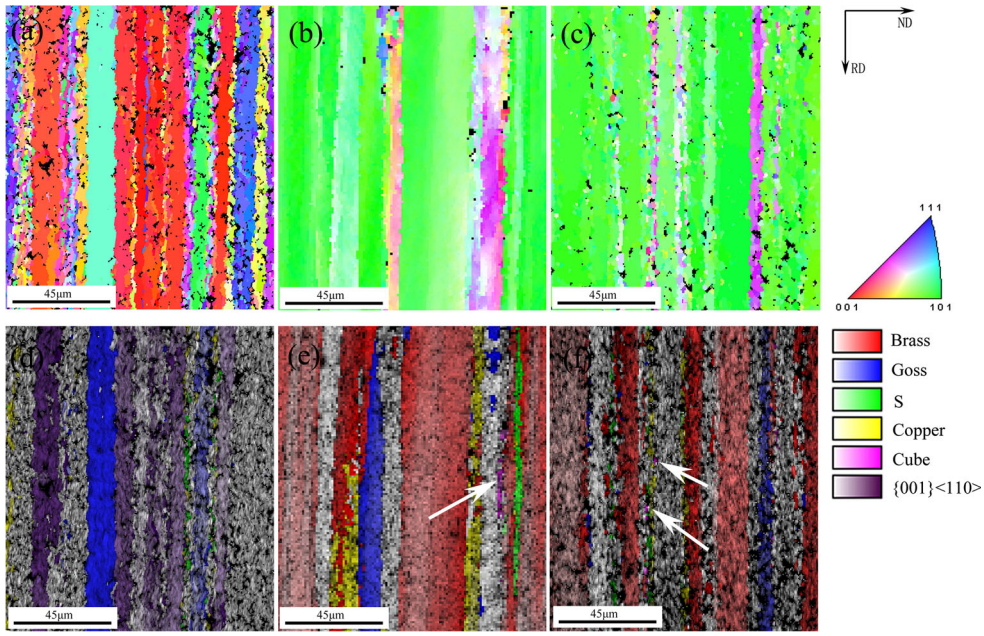

Fig. 12 Orientation distribution maps and corresponding texture distribution maps of hot-rolled Al-Cu-Mg alloy sheets with different rolling reductions at different rolling temperatures: (a) and (d) 90% reduction at 380 °C; (b) and (e) 82% reduction at 495 °C; and (c) and (f) 90% reduction at 495 °C

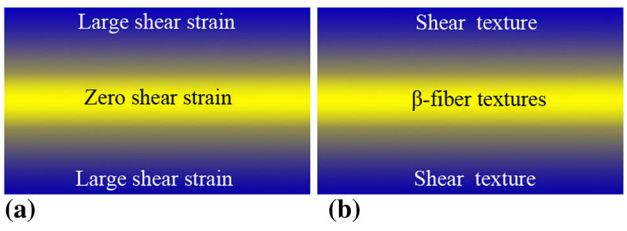

Fig. 13 The shear strain and resultant texture distributions along the thickness direction: (a) the shear strain distribution, (b) the texture distribution

with the increase in rolling passes, resulting in the decrease in the Brass component.

4.3 Development of the Cube Component

The occurrence of recrystallization in the hot rolling means that the Cube-oriented grains should probably appear in the final rolled materials. Due to the weak intensity of the Cube component, the macro-texture measurement result did not clearly show the existence of the Cube texture. However, the Cube-oriented grains were observed apparently in the sheets hot rolled at the high rolling temperature, as shown in Fig. 12.

The small and near equiaxed Cube grains tended to appear in the S or Copper band. It means that Cube grains can be nucleated in S and Copper bands more easily than Brass bands. It was reported that the orientation relation between the Cube and S grains was characterized by a rotation of 37° about $<111>$ axis, close to the classic $40°<111>$ high mobility boundary (Ref 31). This high mobility boundary can promote the oriented nucleation of recrystallized Cube grains (Ref 25, 31, 34). Alvi et al. (Ref 15) found that the Brass texture was difficult to recrystallize, resulting in Cube grains grew more slowly into Brass grains than into S or Copper grains in the pure aluminum. Hence, it is well understood that the Cube grain preferred to develop in the Copper and S bands other in the Brass band.

5. Conclusion

In present paper, the development of hot rolling textures in Al-Cu-Mg alloy has been investigated by x-ray texture measurement and EBSD orientation analysis. This study shows that:

1. As the rolling temperature increases, a texture transition from the shear texture $\{001\}<110>$ to the β-fiber textures occurred in the intermediate layer of hot-rolled Al-Cu-Mg alloy sheets.
2. High rolling temperatures promoted the activation of the non-octahedral $\{112\}<110>$ slip system, consequently enhancing the strength of Brass texture.
3. At the low rolling reduction of 74%, the textures with low intensities tended to converge on the α-fiber, containing Goss, Brass, P and L. As the rolling reduction increased to 90%, the textures were strengthened and gradually flew toward the β-fiber, containing Brass, Copper and S.
4. The recrystallized Cube grains preferred to develop in the S or Copper bands rather than the Brass band.

Acknowledgments

The authors are grateful for financial support from the National Key Research and development Program of China (Grant No. 2016YFB0300900), the National Key Fundamental Research Project of China (2012CB619506-3), National Natural Science Foundation of China (51171209) and 2011 Program of Ministry of Education of China.

Reference

1. J.J. Sidor, R.H. Petrov, and L.I. Kestens, Modeling the Crystallographic Texture Changes in Aluminum Alloys During Recrystallization, *Acta Mater.*, 2011, **59**, p 5735–5748
2. S. Panchanadeeswaran and D.P. Field, Texture Evolution During Plane Strain Deformation of Aluminum, *Acta Mater.*, 1995, **43**(4), p p1683–p1692
3. O. Engler and K. Lacke, Mechanism of Recrystallization Texture Formation in Aluminum Alloys, *Scr. Metal. Mater.*, 1992, **27**, p 1527–1532
4. O. Daaland and E. Nes, Origin of Cube Texture During Hot Rolling of Commercial Al-Mn-Mg Alloys, *Acta Mater.*, 1996, **43**(4), p 1389–1411
5. C. Maurice and J.H. Driver, Hot Rolling Textures of f.c.c. Metals—Part I. Experimental Results on Al Single and Polycrystals, *Acta Mater.*, 1997, **45**(11), p p4627–p4638
6. W.C. Liu and J.G. Morris, Effect of Hot and Cold Deformation on the β Fiber Rolling Texture in Continuous Cast AA 5052 Aluminum Alloy, *Scripta Mater.*, 2005, **52**, p 1317–1321
7. C. Zener and J.H. Hollomon, Effect of Strain Rate Upon Plastic Flow of Steel, *J. Appl. Phys.*, 1944, **15**(1), p 22–32
8. I. Samajdar, P. Ratchev, B. Verlinden, and E. Aernoudt, Hot Working of AA1050—Relating the Microstructural and Textural Developments, *Acta Mater.*, 2001, **49**, p 1759–1769
9. Q. Contrepois, C. Maurice, and J.H. Driver, Hot Rolling Textures of Al-Cu-Li and Al-Zn-Mg-Cu Aeronautical Alloys: Experiments and Simulations to High Strains, *Mater. Sci. Eng., A*, 2010, **527**, p 7305–7312
10. O. Engler, J. Hirsch, and K. Lucke, Texture Development in Al 1.8 wt% Cu Depending on the Precipitation State-I. Rolling Textures, *Acta Metall.*, 1989, **37**(10), p 2743–2753
11. C. Gras, M. Meredith, and J.D. Hunt, Microstructure and texture evolution after twin roll casting and subsequent cold rolling of Al-Mg-Mn aluminium alloys, *Process. Technol.*, 2005, **169**(2), p 156–163
12. H. Tian, H.L. Suo, Y. Liang, and Y. Zhao, Effect of Surface Shear on Cube Texture Formation in Heavy Cold-Rolled Cu-45 at%Ni Alloy Substrates, *Mater. Lett.*, 2015, **141**, p 83–87
13. C.G. Kang, H.G. Kang, H.C. Kim, M.Y. Huh, and H.G. Suk, Formation of Shear Texture, Components During Hot Rolling of AA 1050, *J. Mater. Process. Technol.*, 2007, **187–188**, p 542–545
14. D.H. Shin, I. Kim, J. Kim, and K.T. Park, Grain Refinement Mechanism During Equal-channel Angular Pressing of a Low-Carbon Steel, *Acta Mater.*, 2001, **49**, p 1285–1292
15. M.H. Alvia, S.W. Cheong, J.P. Suni, H. Weiland, and A.D. Rollett, Cube Texture in Hot-Rolled Aluminum Alloy 1050(AA1050)—Nucleation and Growth Behavior, *Acta Mater.*, 2008, **56**, p 3098–3108
16. J. Hjelen, R. Orsund, and E. Nes, On the Origin of Recrystallization Textures in Aluminium, *Acta Metall. Mater.*, 1991, **39**(7), p 1377–1404
17. M.Y. Huh, J.C. Park, and S. Lee, Interpretation of Hot Rolling and Cold Rolling Texture in High Purity Aluminium, *Met. Mater. Int.*, 1996, **2**(3), p p141–p149
18. O. Engler, C.N. Tomé, and M.Y. Huh, A Study of Through-Thickness Texture Gradients in Rolled Sheets, *Metall. Mater. Trans. A*, 2000, **31**(9), p 2299–2315
19. M.Y. Huh, K.R. Lee, and O. Engler, Evolution of Texture and Strain States in AA3004 Sheet During Rolling with a Dead Block, *Int. J. Plast*, 2004, **20**, p 1183–1197
20. Z. Wusatoski, *Fundament and of Rolling*, Oxford University Press, Oxford, 1960, p 153–161
21. O. Pawelski, W. Rasp, and C. Hoerster, Ring Compression Test as Simulation Test for the Investigation of Friction in Hot Metal Forming, *Steel Res.*, 1989, **60**, p 395–402
22. S. Venugopal, G. Srinivasan, S. Venkadesan, and V. Seetharaman, A Note on the Determination of the Friction Factor by Means of the Reduction-Capacity Test, *J. Mech. Work Technol.*, 1989, **19**(2), p p261–p266
23. J.G. Lenard, The Effect of Temperature on the Coefficient of Friction in Flat Rolling, *CIRP Ann. Manuf. Technol.*, 1991, **40**(1), p 223–226
24. H.P. Yang, Y.H. Sha, F. Zhang, and L. Zuo, Through-Thickness Shear Strain Control in Cold Rolled Silicon Steel by the Coupling Effect of Roll Gap Geometry and Friction, *J. Mater. Process. Technol.*, 2010, **210**, p 1545–1550
25. H.E. Vatne, R. Shahani, and E. Nes, Deformation of Cube-Oriented Grains and Formation of Recrystallized Cube Grains in a Hot Deformed Commercial AlMgMn Aluminium Alloy, *Acta Mater.*, 1996, **44**(11), p 4447–4462
26. A. Duckham, R.D. Knutesn, and O. Engler, Influence of Deformation Variables on the Formation of Copper-Type Shear Bands in Al-1Mg, *Acta Mater.*, 2001, **49**, p 2739–2749
27. C. Maurice and J.H. Driver, Hot Rolling Textures of f.c.c. Metals—Part II. Numerical Simulations, *Acta Mater.*, 1997, **45**(11), p 4639–4649
28. F. Pérocheau and J.H. Driver, Texture Gradient Simulations for Extrusion and Reversible Rolling of FCC Metals, *Int. J. Plast*, 2000, **16**, p 73–89

29. M. Carrard and J.L. Martin, A Study of (001) Glide in [112] Aluminium Single Crystals, *Philos. Mag. A*, 1988, **58**, p 391–405
30. Q. Zhao, Z. Liu, S. Li, T. Huang, P. Xia, and L. Lu, Evolution of the Brass Texture in an Al-Cu-Mg Alloy During Hot Rolling, *J. Alloys Compd.*, 2017, **691**, p 786–799
31. M.C. Theyssiera and J.H. Driver, Recrystallization Nucleation Mechanism Along Boundaries in Hot Deformed Al Bicrystals, *Mater. Sci. Eng., A*, 1999, **272**, p 73–82
32. P.S. Bate, Y. Huang, and F.J. Humphreys, Development of the "Brass" Texture Component During the Hot Deformation of Al-6Cu-0.4Zr, *Acta Mater.*, 2004, **52**, p 4281–4289
33. W.T. Read and W. Shockley, Dislocation Models of Crystal Grain Boundaries, *Phys. Rev.*, 1950, **78**, p 275–289
34. O. Engler, H.E. Vatne, and E. Nes, The Roles of Oriented Nucleation and Oriented Growth on Recrystallization Textures in Commercial Purity Aluminium, *Mater. Sci. Eng., A*, 1996, **205**, p 187–198